SYNOPSIS

of Ph.D thesis entitled

AERODYNAMIC DRAG AND LIFT CHARACTERISTICS OF A NEWLY DEVELOPED ELLIPTICAL-BLADED SAVONIUS WIND TURBINE ROTOR

Proposed to be Submitted in Partial Fulfillment
of the Requirements for the Degree of

DOCTOR OF PHILOSOPHY

BY

Md. Nur Alom

DEPARTMENT OF MECHANICAL ENGINEERING
INDIAN INSTITUTE OF TECHNOLOGY GUWAHATI
GUWAHATI – 781039, INDIA

The fossil fuel resources and the environmental effect of their use necessitate a change to renewable energy sources in the near future which is pollution free, eco-friendly, low cost and ease of availability. However, among all the renewable energy, wind is easily available and eco-friendly. In the recent times, wind energy has become the world fastest increasing resource of renewable energy. Wind turbines are used to converts the kinetic energy of wind into the mechanical and electrical work. Historically, the earliest known wind turbines were found in Sistan, the eastern province of Iran during 9th century. These machines, then known as windmills, relied on drag forces for their operation and were primarily used for grain grinding or pumping water (Gupta, 2015). The engineering aspects of these Sistan machines are hardly documented and reported in literature. With some changes in the design, these machines were used in the production of electricity during late 19th century. A further design was evolved in 1925 when the Finnish engineer S. J. Savonius used two or more S shaped cups/buckets that rotated on a vertical axis where the wind is perpendicular to the buckets. This drag-based Savonius vertical-axis wind turbine (*VAWT*) has a lesser efficiency but it has the advantages of design simplicity, lower installation and maintenance cost, good self-starting capability (Owaga et al., 1989; Modi and Fernando, 1989; Plourde et al., 2012; Wong et al., 2017), insensitive to wind direction and absence of yaw mechanism. The efficiency of this turbine, known as power coefficient (C_p) has risen from 0.11 to 0.33 depending upon the type of buckets/blades used. The C_P of the rotor further can be increased by incorporating augmentation techniques such as deflector plate, curtains, nozzle, wind shields, venting and others. Unlike the Savonius turbine, the Darrieus turbine is a lift-based machine. The other category of lift-based turbines that rotate on a horizontal-axis where the wind is parallel to the blades are known as horizontal-axis wind turbines (*HAWTs*). Although the lift-based *HAWTs* have higher efficiency but it has required tall and robust structure, yaw mechanism (Menter, 2004; Dossena et al., 2015). Hence, the manufacture cost is more in *HAWTs*. Based on aerodynamic forces, the *VAWTs* are categorized into the lift- and drag-based devices. The drag-based rotors are Savonius and Sistan rotors; whereas, the lift-

based rotors include H- and Darrieus rotors. Although the drag-based rotors have better self-starting capabilities than the lift-based *VAWT*s, they have lesser C_P. Savonius rotor operates mainly on drag force (D_f), but it also experiences a lesser amount of lift force (D_L).

The basic parameters and forces of a two-bladed Savonius rotor are shown in Fig. 1. A wind turbine converts the kinetic energy of the wind into torque acting on the rotor blades. The amount of energy which the wind transfers to the rotor depends on the density of the air, the rotor area, and the wind speed. The performance of the Savonius rotor is usually estimated by the two performance parameters such as torque coefficient (C_T) and power coefficient (C_P) (Emmanuel and Jun, 2011) and can be expressed as

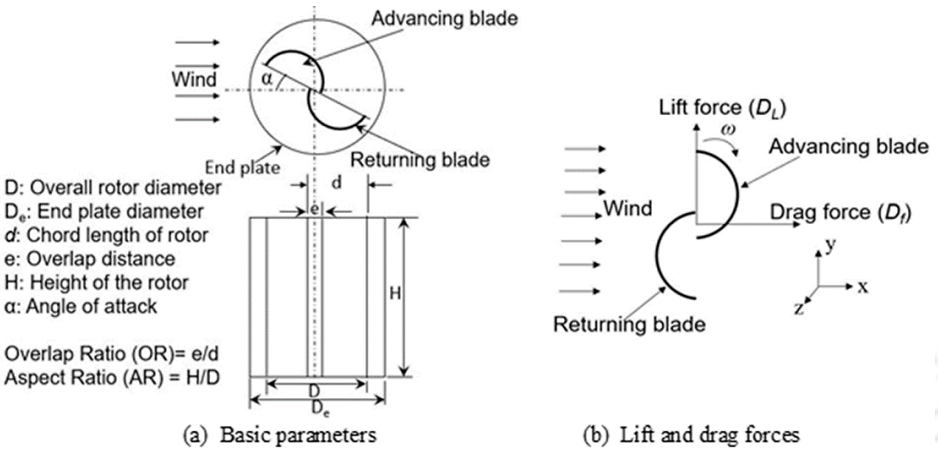

Fig. 1: Illustration of basic parameters and forces of Savonius rotor

After the open literature review, it is supposed that the Savonius rotor can be a viable option for off grid energy conversion in certain cases of confined space and low wind speed region, where other types of turbines cannot work efficiently. However, the existing design is yet a matter of research to make it more useful in particular situations. In view of this, the objective of the present investigation is to investigate the aerodynamic drag and lift characteristics of a newly developed elliptical-bladed Savonius rotor to improve its torque and power coefficient (C_T and C_P) by considering the various geometric and aerodynamic parameters. Though the Savonius rotor is a drag-based device, a minor amount of lift force also contributes to its C_T and C_P. The vent augmentation technique is also incorporated with the optimized Savonius rotor to improve its performance further. The following roadmap (Fig. 2) shows how the objective has been established and how the improvement of the turbine has been brought about through numerical simulations and wind tunnel experiments.

Initially, 2D unsteady simulations are carried out using ANSYS Fluent for the elliptical profile with sectional cut angle (θ) = 47.5°, modified Bach, Benesh and semicircular profile to found the optimum blade profile for Savonius rotor. The rotor blades have been discretization with unstructured triangular grids in ANSYS meshing (Fig. 3). This is because unstructured mesh methods logically offer the possibility of incorporating adaptivity. Also, it offers flexibility in generating a mesh flow domain for a complex flow problem. The domain consists of two sections, viz., the outer rectangular stator and the inner circular rotor. The two sections are separated by a sliding interface. The details of the meshing and boundary conditions are in Fig. 4. After the grid and time independent test the grid with 169900 elements and 1°/step is chosen to 2D simulations. Past studies conducted by several investigators reveal that the *SST k-ω* model has better prediction capabilities (Menter, 2004; Plourde, 2012). Hence, this model has been considered for all the simulations.

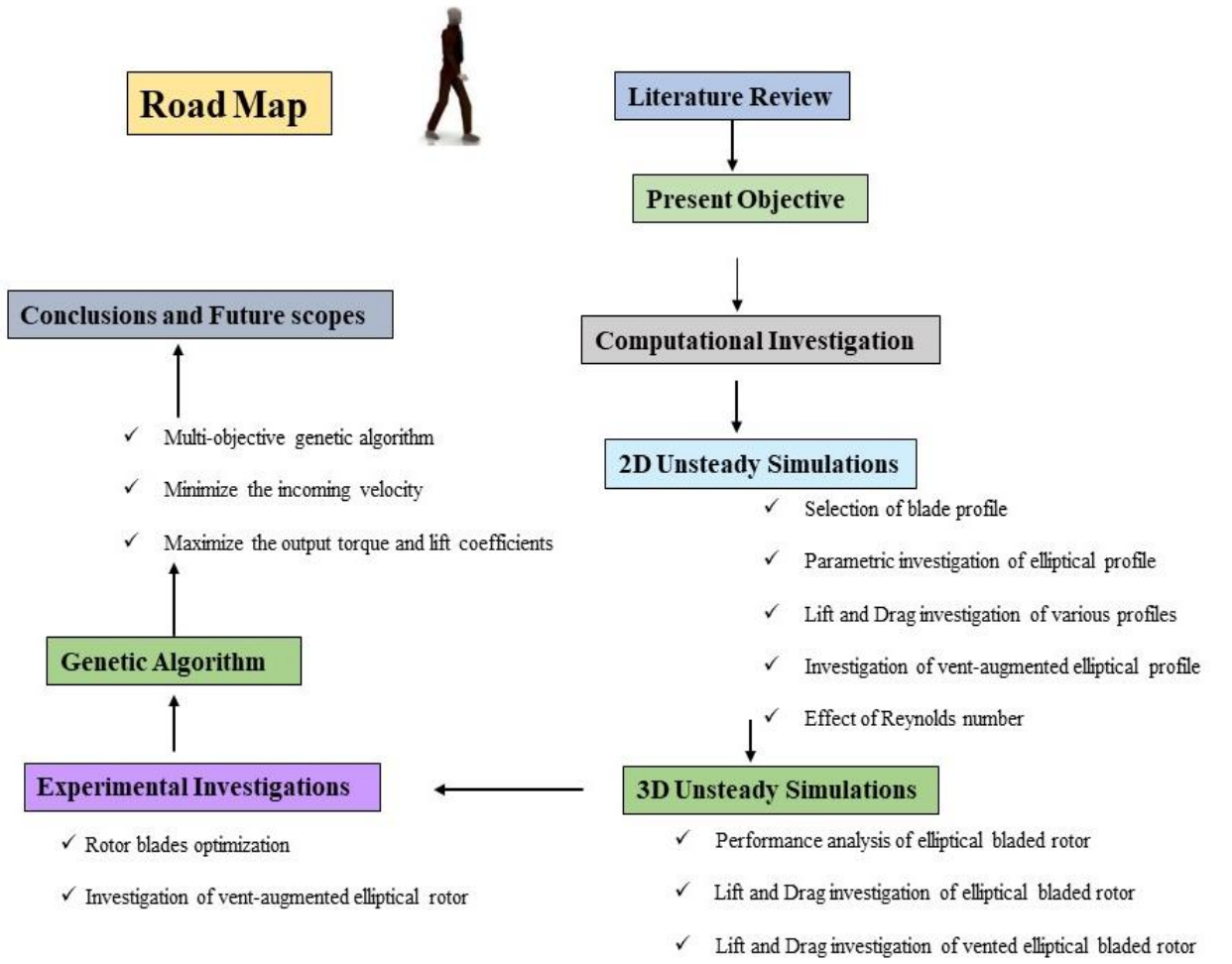

Fig.2: Roadmap of PhD research work

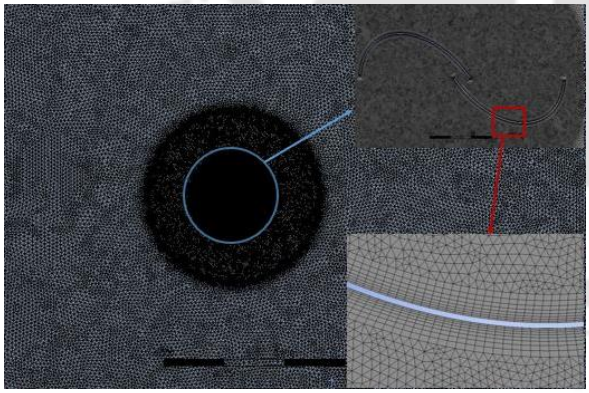

Fig. 3: Mesh generation around the rotor

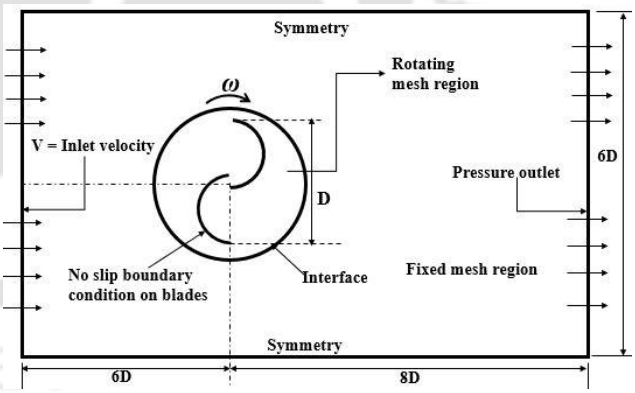

Fig. 4: Boundary Conditions and Computational Domain.

From the numerical analysis, the peak C_P of 0.34 is obtained for the elliptical profile at *TSR* = 0.80; whereas at the same *TSR*, the peak C_P is found to be 0.27, 0.29 and 0.30 for the semicircular, Benesh and modified Bach profiles, respectively (Fig. 5). Thus, there is an improvement of C_P in the elliptical profile than the semicircular, Benesh and modified Bach profiles by 26%, 17% and 13%, respectively.

From Fig.6, it has been predicted that a higher velocity magnitude and lesser tip losses in elliptical profile than the other profiles. Also, the improved over lapping flow is found in elliptical profile than the other profile.

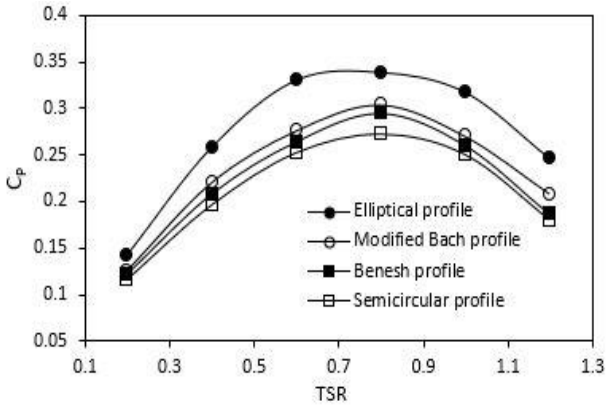

Fig. 5: Performance coefficients obtained from 2D numerical simulation

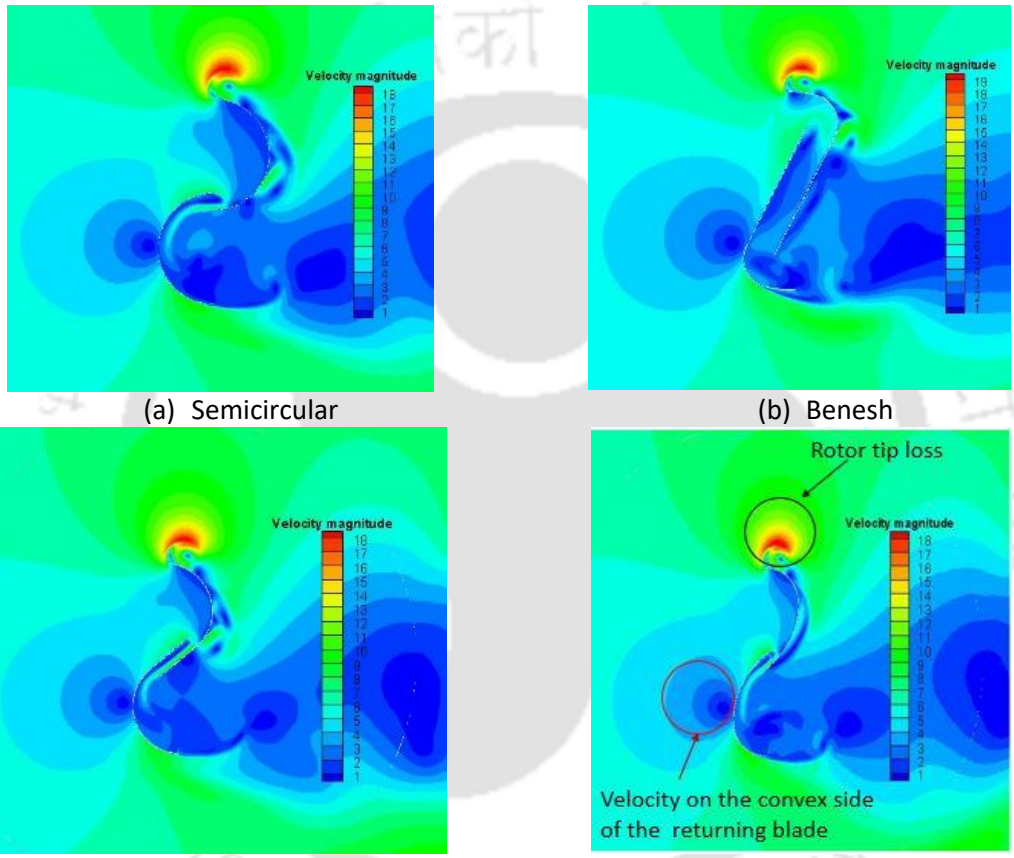

(a) Semicircular (b) Benesh

(c) Modified Bach (d) Elliptical

Fig. 6: Velocity magnitude (m/s) of various rotor profile at TSR = 0.80

2D unsteady simulations are also carried out for the newly developed elliptical profile to found its optimum geometric parameters such as overlap ratio, number rotor blades and effect of shaft and Reynolds number. From the numerical results, it has been observed that the 2-bladed elliptical profile with overlap ratio (*OR*) = 0.15 has the maximum power coefficient at TSR = 0.80. The 2-bladed profile shows a peak C_P of 0.34, whereas for the 3- and 4-bladed profiles, the peak C_P is found to be 0.29 and 0.24, respectively (Fig. 7). With the presence of shaft, the power coefficients of the 2-bladed system are reduced because of the reduction in overlapping flow. The peak C_P is found to be 0.31 for the 2-bladed elliptical profile in the presence of the central shaft (Fig. 8).

The rotor profiles have been tested numerically at various Reynolds number, *Re* =0.72 x10^5, 0.89 x 10^5 and 1.01 x 10^5 corresponding to the wind speeds of 5 m/s, 6.2 m/s and 7 m/s. Usually, the C_P of the rotor is increased with the increased in *Re*.

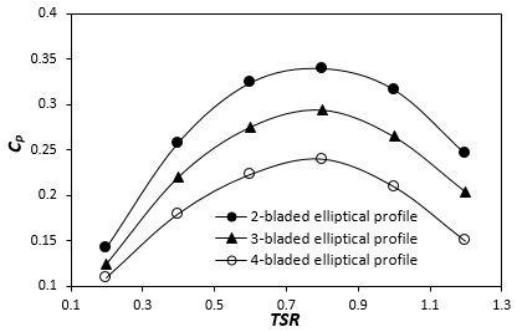

Fig. 7: C_P vs *TSR* for 2-, 3- and 4-bladed elliptical profile

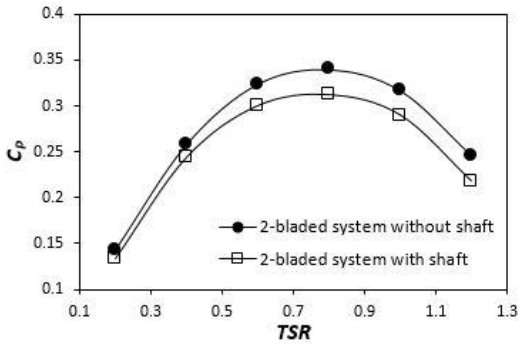

Fig. 8: C_P vs *TSR* for the elliptical-bladed profile without and with shaft

To arrive at a suitable design configuration, C_L and C_D has to be investigated, hence 2D unsteady simulations are conducted for the elliptical, modified Bach, Benesh and semicircular profiles. C_L and C_D are also investigated for the vented elliptical and semicircular profile. Initially, the present 2D unsteady results have been validated with of the unsteady results of Roy and Ducoin, (2016) at the identical conditions (Fig. 9).

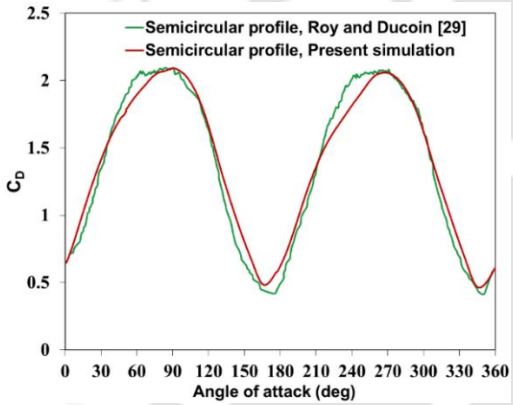

Fig. 9: Validation of present 2D C_D with the available results.

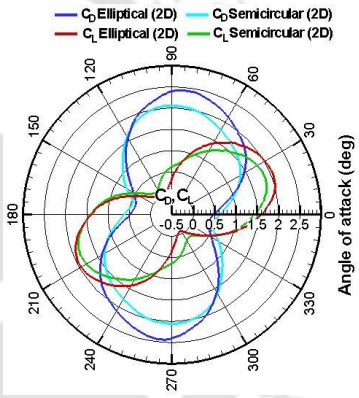

Fig.10: Variation of C_D and C_L for the elliptical and semicircular profiles at *TSR* = 0.6.

From the 2D unsteady simulations, the C_{Dmax} for elliptical-profile is found to be 2.43 at α = 84° and 266° respectively; however, for the semicircular profile, C_{Dmax} is 2.07 corresponding α =91° and 270°. Hence, there is an improvement in C_{Dmax} of 17.4% in elliptical profile than the semicircular profile (Fig. 10). The average C_D for a complete rotation of elliptical and semicircular profile is found to be 1.43 and 1.35, respectively. Hence, there is higher average C_D by 6% in the elliptical profile than the semicircular profile. The average C_D of modified Bach and Benesh are found to be 1.41, 1.25, respectively. Hence, in modified Bach profile, there is an improvement of C_D by 4.5% than the semicircular profiles. Also, the average C_D for vented elliptical and semicircular profiles are found to be 1.45 and 1.39, respectively. Thus, there is an increase in average C_D by 1.4% and 3% in the vented elliptical and semicircular profile than the non-vented elliptical and semicircular profile.

The 3D unsteady simulations are carried out with the vented elliptical-bladed rotor, and results are compared with the non-vented elliptical-bladed rotor at V = 6.2 m/s. The performance coefficients are calculated at rotating conditions. The flow physics are also investigated around the vented and non-vented elliptical bladed rotor at an aspect ratio (AR) = 0.70. The C_L and C_D of the vented and non-vented elliptical bladed rotor have been calculated to arrive at the optimum design configuration. The 3D unsteady results have been validated with that of the available results of Jaohindy et al., (2013) at the identical conditions. From the 3D unsteady simulation, the C_D and C_L are estimated for elliptical and

semicircular bladed rotors at *TSR* = 0.6 and AR = 1.09. The average C_D for the elliptical-bladed rotor is 1.31 and for the semicircular bladed rotor is 1.26. Thus, there is an improvement in average C_D by 4% in elliptical bladed rotor than the semicircular bladed rotor. The maximum C_D is found to be 2.18 and 2.19 at α =70° and 249°, respectively for the elliptical bladed rotor, while, for the semicircular-bladed rotor, the maximum C_D is found to be 1.83 and 1.85 at α = 64° and 244° (Fig. 11). The velocity magnitude is found to be maximum in the advancing surface of the elliptical bladed rotor than the semicircular bladed rotor (Fig. 12). With the incorporation of vent-augmenter, there is a marginal improvement in average C_D in elliptical bladed rotor. The average C_D for the vented elliptical and semicircular bladed rotors is found to be 1.32 and 1.28, respectively. The average C_L for the vented elliptical bladed rotors is found to be 0.51. Thus, there is an increase of average C_L by 6.3% in elliptical-bladed rotor with vents than the same rotor without vents. The average C_L for the vented semicircular bladed rotors is found to be 0.53, respectively.

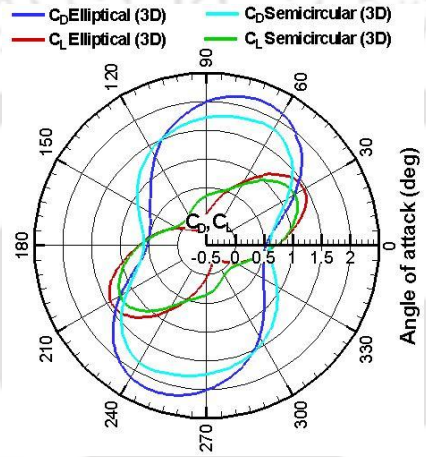

Fig.11: Variation of the 3D C_D and C_L for the elliptical and semicircular-bladed rotors at *TSR* = 0.6.

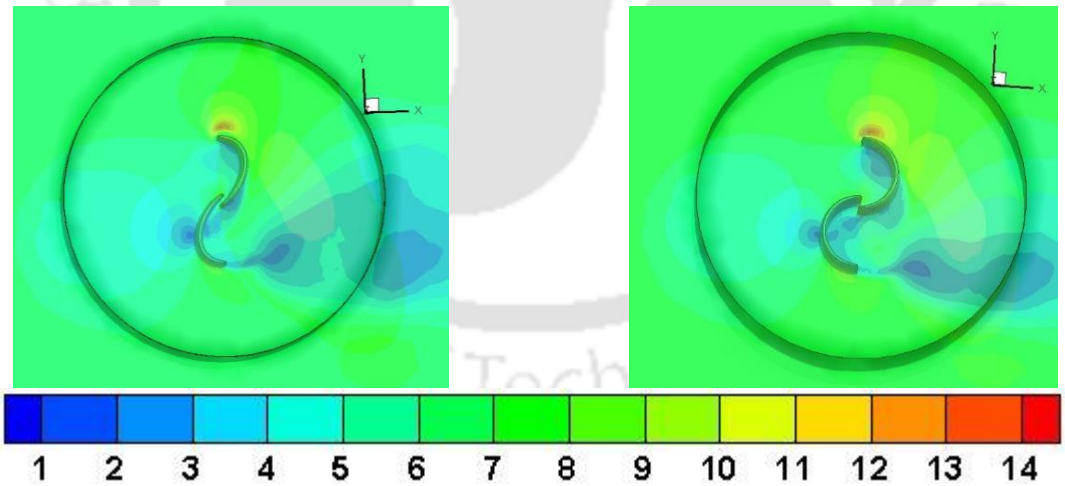

Fig.12: Velocity magnitude (m/s) contours of elliptical and semicircular bladed rotors at *TSR* = 0.6

After the series of 2D and 3D unsteady simulations, the wind tunnel experiments are performed for the elliptical, modified Bach, Benesh rotor to validate the numerical results. The experiments are conducted for the semicircular bladed rotor at the identical conditions to have a direct comparison. Further, the experiments are also conducted for the vented elliptical bladed rotor to investigate its influence on the rotor performance. The schematic diagram of a wind tunnel is shown in Fig. 13. The wind turbine blades for this experiment are manufactured using 0.5 mm thick *GI* (Galvanized Iron) sheets with an aspect ratio of 0.7 and 1.09. This material is strong enough to withstand the flow-field of the wind

ranging from 0 to more than 10 m/s. The vented elliptical-bladed rotor is manufacture with AR = 0.7. The error analysis, uncertainty analysis and a suitable blockage correction factor also considered for all the experimental data. The experimental peak C_P values for the elliptical-bladed and semicircular-bladed rotors are found to be 0.19 and 0.15 at *TSR* = 0.7 (Fig. 14); whereas the peak C_P for Benesh and modified Bach rotors are found to be 0.16 at *TSR* = 0.6 and 0.8, respectively. Thus, the elliptical-bladed rotor shows an improvement of C_P by 27% as compared to the semicircular-bladed rotor. With the inclusion of blockage correction, the C_{pmax} is found to be 0.185 for elliptical-bladed rotor at *AR* = 1.09, while for the semicircular bladed rotor is found to be 0.146 at the same AR. The blockage corrected C_{pmax} for the Benesh and modified Bach rotors are found to be 0.156 (Fig. 15).

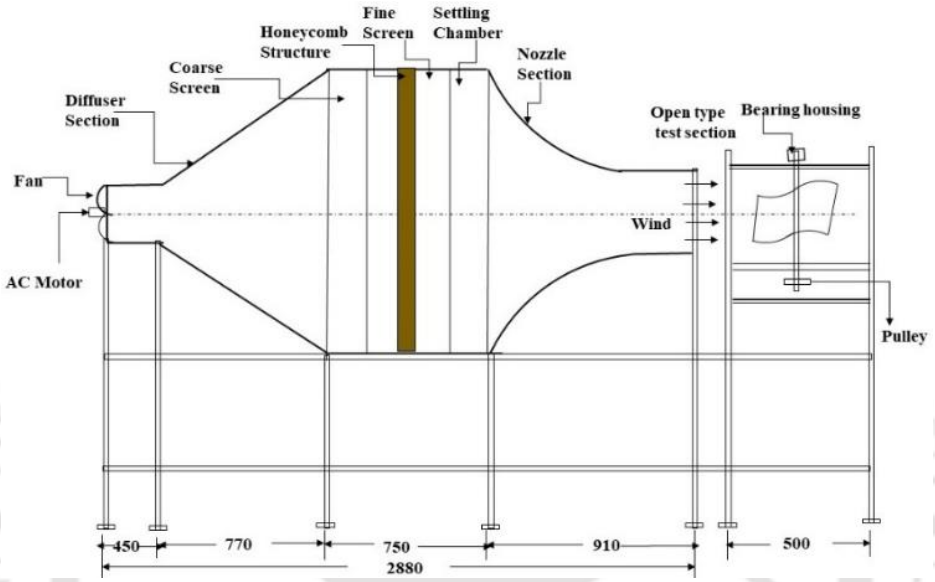

Fig. 13: Schematic diagram of a wind tunnel.

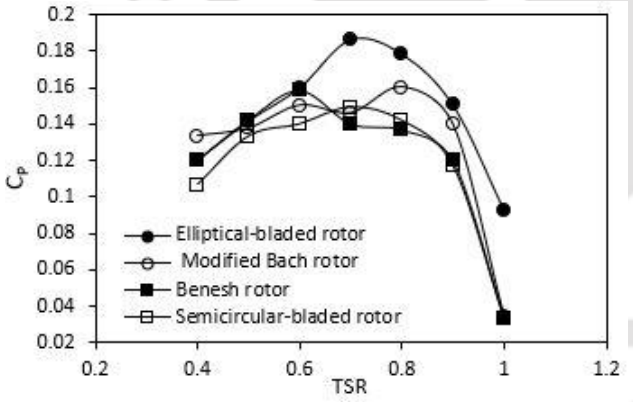

Fig. 14: Performance coefficients obtained from wind tunnel experiments

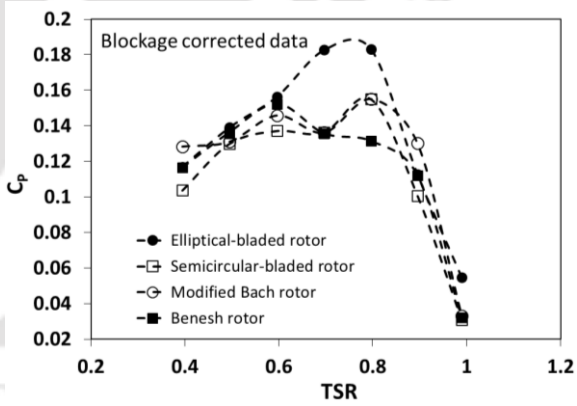

Fig. 15: Blocakge corrected performance coefficient.

Finally, the genetic algorithm has been performed using ANSYS 17.1 direct optimization technique for the 2D geometric model of elliptical and semicircular profiles. Finally, multi-objective genetic algorithm (MOGA) has been carried out with the objective is to minimize the incoming velocity and to maximize the torque and lift coefficients of the elliptical and semicircular bladed profiles for the given incoming velocity of 6.2 m/s. From the MOGA, at TSR = 0.80, the elliptical bladed Savonius rotor shows that the C_P = 0.35 at V = 5.91 m/s. For the semicircular bladed profile, the C_P = 0.28 at V = 6.06 m/s. However, from the unsteady numerical simulation for the elliptical profile, the C_P = 0.34 at V=6.2 m/s and for the semicircular profile C_P = 0.27 at V=6.2 m/s. Thus, the newly developed elliptical bladed Savonius rotor is the better contender for small scale power generation in rural areas.

References

Dossena, V., Persico, G., Paradiso, B., Battisti, L., Dell'Anna, S., Brighenti, A., and Benini, E., 2015, "An Experimental Study of the Aerodynamics and Performance of a Vertical Axis Wind Turbine in a Confined and Unconfined Environment," ASME J. Energy Resour. Technol., 137(5), p. 51207.

Emmanuel, B., and Jun, W., 2011, "Numerical study of a six-bladed Savonius wind turbine," ASME J. Sol. Energy Eng., 133(4), p. 44503.

Gupta, A.K., 2015. Efficient wind energy conversion: Evolution to modern design. Journal Energy Resourse Technology. 137, 51201.

Jaohindy, P., McTavish, S., Garde, F. and Bastide, A., 2013. An analysis of the transient forces acting on Savonius rotors with different aspect ratios. Renewable Energy, 55, pp. 286-295.

Menet, J. L., 2004, "A double-step Savonius rotor for local production of electricity: A design study," Renew. Energy, 29(11), pp. 1843–1862.

Modi, V., and Fernando, M., 1989, "On the performance of the Savonius wind turbine," ASME J. Sol. Energy Eng., 111(1), pp. 71–81.

Plourde, B. D, Abraham, J. P, Mowry, G., and Minkowycz, W., 2012, "Simulations of Three-Dimensional Vertical-Axis Turbines for Communications Applications," Wind Engineering, Vol. 36, pp. 443-454.

Roy, S., Ducoin, A., 2016. Unsteady analysis on the instantaneous forces and moment arms acting on a novel Savonius-style wind turbine. Energy Conversion Management, 121, 281–296.

Wong, K. H., Chong, W. T., Sukiman, N. L., Poh, S. C., Shiah, Y.-C., and Wang, C.-T., 2017, "Performance enhancements on vertical axis wind turbines using flow augmentation systems: A review," Renew. Sustain. Energy Rev., 73(February), pp. 904–921.

List of Publications

Journals

1. **Alom, N**., and **Saha, U.K**., 2019. "Examining the Aerodynamic Drag and Lift Characteristics of a Newly Developed Elliptical- Bladed Savonius Rotor," ASME Journal of Energy Resources Technology, Vol. 141, No. 5, pp: 051201-051201-12.
2. **Alom, N**., and **Saha, U.K.,** 2019, "Evolution and Progress in the Development of Savonius Wind Turbine Rotor Blade Profiles and Shapes," ASME Journal of Solar Energy Engineering, Vol. 141, No.3, pp: 030801-1-030801-15.
3. **Alom, N**., and **Saha, U.K.,** 2019, "Drag and lift characteristics of a novel elliptical-bladed Savonius rotor with vent augmenters," ASME Journal of Solar Energy Engineering, Vol. 141, No. 5, pp: 051007-1-051007-12.
4. **Alom, N**., and **Saha, U.K.,** 2019, "Influence of blade profiles on Savonius rotor performance: Numerical simulation and experimental validation," Energy Conversion and Management, Vol. 186, pp: 267-277
5. **Alom, N**., and **Saha, U.K**., 2018. "Four decades of research into the augmentation techniques of Savonius wind turbine rotor," ASME Journal of Energy Resources Technology, Vol. 140, No. 5, pp: 050801-1-050801-14.
6. **Alom, N.,** and **Saha, U.K**., 2018. "Performance analysis of a vent-augmented elliptical-bladed Savonius rotor by numerical simulation and wind tunnel experiments," Energy, Vol. 152, pp: 277-290.
7. **Alom, N., Borah, B**., and **Saha, U. K**., 2018, An insight into the drag and lift characteristics of modified Bach and Benesh profiles of Savonius rotor, Energy Procedia, Vol. 144, pp: 50-56. Presented at the *4th International Symposium on Hydrogen Energy, Renewable Energy and Materials* (HEREM), June 13 – 14, Bangkok, Thailand.

International Conferences

1. **Alom, N.,** and **Saha, U.K**., 2019, "Analyzing the effect of shaft and end-plates of a newly developed elliptical-bladed Savonius rotor from wind tunnel tests," Paper No. OMAE2019-95570, ASME 38th International Conference on Ocean, Offshore and Arctic Engineering, June 9-14, 2019, Glasgow, Scotland, UK**. (Accepted)**
2. **Alom, N., and Saha, U.K.,** 2017. "Arriving at the optimum overlap ratio for an elliptical-bladed Savonius rotor," Paper No. GT2017-64137, ASME Turbo Expo, June 26–30, Charlotte, North Carolina, USA.
3. **Alom, N., Kumar, N** and **Saha, U.K.**, 2017. "Aerodynamic performance of an elliptical-bladed Savonius rotor under the influence of number of blades and shaft," Paper No. GTIndia2017-4554, ASME Gas Turbine India Conference, December 7–8, Bangalore, India.
4. **Alom N.,** and **Saha U.K.,** 2016, "Numerical Optimization of Semicircular-bladed Savonius Rotor using Vent Augmenters", Asian Congress on Gas Turbines 2016, November 14-16, IIT Bombay, Mumbai, India.